

A sequential dimerization mechanism for erythropoietin receptor activation

DAVID J. MATTHEWS*, ROBERT S. TOPPING, ROBERT T. CASS, AND LUTZ B. GIEBEL

Department of Receptor Biology, Arris Pharmaceutical Corporation, South San Francisco, CA 94080

Communicated by Harvey F. Lodish, Whitehead Institute for Biomedical Research, Cambridge, MA, June 11, 1996 (received for review May 1, 1996)

ABSTRACT We have probed the interaction of human erythropoietin (EPO) with its receptor (EPO-R) by analyzing a panel of 17 EPO mutants in a variety of *in vitro* assays. Mutant proteins were expressed in 293s cells and quantified by using an N-terminal epitope tag in conjunction with a surface plasmon resonance assay. Receptor binding was studied using both a soluble form of the EPO-R extracellular domain in an ELISA-format binding competition assay and full-length EPO-R in transfected BaF3 cells. Proliferative activity of the mutants was also determined in the BaF3-derived cell line and was correlated with the results from binding assays. Based on the results of these assays, we identified two distinct receptor binding sites on the EPO molecule. We propose that one site, containing residues Arg-150 and Lys-152, binds initially to EPO receptor on the cell surface. A second site, containing Arg-103 and Ser-104 (and possibly Arg-14), is involved in binding a second EPO-R at the cell surface, thus forming a homodimeric receptor complex. Furthermore, we demonstrate that one EPO mutant (R103A), which has previously been shown to lack proliferative function, is in fact an EPO antagonist. Taken together, these data support a sequential dimerization mechanism of EPO-R activation.

Human erythropoietin (EPO) is a 166-aa glycoprotein that is involved in the proliferation and differentiation of erythroid progenitor cells (1). These cellular responses are mediated by the EPO receptor (EPO-R), a 508-aa glycoprotein containing a single transmembrane domain (2) that has been classified as a member of the growth hormone subfamily of class I cytokine receptors (3). Several studies have implicated receptor dimerization in the EPO signal transduction mechanism. For example, a constitutively active variant of EPO-R has been isolated, containing an arginine to cysteine mutation at position 129 in the receptor extracellular domain (4). The R129C mutant receptors have been shown to form disulfide-linked dimers in plasma membranes (5), and several similar cysteine mutations have been discovered that render the receptor constitutively active (6). EPO-R has also been coexpressed with inactive EPO-R analogs that lack most of the cytoplasmic domain, revealing a dominant inhibitory effect of the inactive receptor on proliferative activity of the wild-type (WT) receptor (6, 7). Recent biophysical studies (8) have also suggested that EPO binds to two receptor molecules, one with high affinity (≈ 1 nM) and one with low affinity (≈ 1 μ M). Furthermore, recent studies in our laboratory have shown that EPO can form a complex in solution with two molecules of the EPO-R extracellular domain (H. Zhan, personal communication), and that a bivalent monoclonal antibody raised against the extracellular domain of EPO-R is capable of transducing a proliferative signal in an EPO-dependent cell line (H. Schneider, personal communication). These findings will be published elsewhere.

Although dimerization of EPO-R at the cell surface has not been directly observed, we sought to explore the EPO-R activation mechanism in terms of a sequential dimerization model, as has been described for human growth hormone (hGH) receptor. X-ray crystallography (9) and other biophysical techniques (10) have demonstrated that one hGH molecule binds to two receptor molecules, and mutagenesis studies (11–13) have revealed important receptor binding determinants on hGH. hGH binds initially to one receptor via residues comprising “site 1” on the hormone. A second receptor binding site (“site 2”) is subsequently involved in a receptor dimerization event on the cell surface.

Previous EPO mutagenesis studies have largely concentrated on identifying mutants that affect cell proliferation (14–16). Here, we investigate the nature of the proposed dimerization event in EPO-R activation and identify several EPO mutants that define site 1 and site 2 for EPO-R binding. We constructed a panel of 17 EPO mutants and used a sensitive biosensor method to determine the mutant protein concentrations. To decouple receptor binding and receptor activation events, we measured the activity of mutant proteins by using several different techniques: an *in vitro* proliferation assay and an ELISA format assay. We also assessed the cell binding activities of several mutants using a cell binding assay. Our results show that the sequential dimerization hypothesis is supported by binding and proliferative activities of the mutant proteins in these assays. Moreover, we demonstrate that one mutant, R103A, is completely deficient in site 2 EPO-R binding and is an antagonist of EPO activity.

MATERIALS AND METHODS

Cloning of EPO and Construction of EPO Expression Vector. EPO cDNA was cloned from human fetal liver. First-strand cDNA was synthesized from 1 μ g of poly(A) selected human fetal liver RNA (Clontech) by using a cDNA synthesis kit (Pharmacia), and used as a template to amplify the EPO gene using PCR with oligonucleotide primers 5'-GGAAGCTTATGGGGGTGCACGAATGTC and 5'-CCTCTAGATCATCTGTCCCCTGTCTCTG. Thirty-five PCR cycles were performed using *Taq* DNA polymerase (Roche Molecular Systems, Branchburg, NJ), with each cycle consisting of 0.5 min at 94, 1 min at 50, and 2 min at 72°C. The amplification product was purified and cloned into the polylinker of pcDNA1/amp (Invitrogen), creating the vector pcDNA1/amp.EPO. Nucleotide sequence analysis showed that the sequence of the EPO cDNA obtained was identical to that previously published (17, 18).

Abbreviations: EPO, erythropoietin; EPO-R, erythropoietin receptor; EPObp, extracellular domain of EPO-R; WT, wild-type; hGH, human growth hormone. [Single mutants are designated by the wild-type residue (single-letter amino acid code) followed by its sequence position and the mutant residue. For example, R103A represents a mutant where Arg-103 is changed to alanine.]

*To whom reprint requests should be addressed.

The publication costs of this article were defrayed in part by page charge payment. This article must therefore be hereby marked “advertisement” in accordance with 18 U.S.C. §1734 solely to indicate this fact.

Site-Directed Mutagenesis. Synthetic oligonucleotides for site-directed mutagenesis were obtained from Keystone Laboratories (Menlo Park, CA). An epitope tag sequence encoding the pentapeptide YGGFL was introduced at the N terminus of the EPO protein (between the leader sequence and the mature protein) by mutagenesis according to the method of Kunkel (19).

Single amino acid mutants of EPO were also prepared by using the same technique. Each mutation was confirmed by DNA sequencing by using an Applied Biosystems model 377 DNA sequencer. High purity DNA for mammalian transfections was prepared using a Qiagen plasmid preparation kit (Qiagen, Chatsworth, CA).

Expression of EPO Mutants in 293s Cells. Transient transfections of mutant EPO constructs were performed in 293s cells (ATCC CRL 1573) by the CaPO₄ coprecipitation method (20). The EPO constructs were cotransfected with the pAdVantage vector (Promega) in an attempt to enhance transient protein expression. Transfected cells in 15-cm plates were incubated with 20 ml serum-free 50:50 DMEM/F12 medium for 72 h, after which the medium was collected, centrifuged at ≈ 1000 rpm for 5 min, filtered, and concentrated 10- to 25-fold in Macrosep 10K centrifugal concentrators (Filtron Technology, Northborough, MA).

Quantitation of Mutant Proteins. Mutant proteins with an N-terminal epitope tag (YGGFL) were quantitated by surface plasmon resonance using a BIAcore system (21). The BIAcore 2000 system, CM-5 sensor chip, surfactant P₂₀, and amine coupling kit were obtained from Pharmacia Biosensor (Uppsala). The anti-EPO monoclonal antibody (mAb) D11 and purified WT EPO were gifts from Amgen Biologicals. mAb 3E7 was purchased from Gramsch Laboratories (Schwabhausen, Germany). All injections on the BIAcore sensor chip surface were at a flow rate of 5 μ l/min (unless otherwise stated) and a temperature of 25°C. Between injections of reagents, the sensor chip was continuously washed with 10 mM Hepes (pH 7.3), 150 mM NaCl, 3.4 mM EDTA, and 0.005% surfactant P₂₀. Approximately 7700 resonance units of mAb D11 were coupled to the sensor chip using amine immobilization chemistry (22). The mAb D11 surface was regenerated by using 1-min injections of 1 M formic acid between sample injections. A WT EPO standard curve was generated by injecting WT EPO at various concentrations in triplicate and plotting initial rates of binding versus WT EPO concentration. The concentration of WT YGGFL-EPO was obtained by interpolation of its initial binding rate from the linear standard curve. Next, ≈ 7200 resonance units of the anti-YGGFL antibody mAb 3E7 were immobilized as described above. The mAb 3E7 surface was regenerated by using 50 μ l injections of 10 mM 3-(cyclohexylamino)-1-propanesulfonic acid (CAPS) (pH 10.4) at 50 μ l/min between sample injections. A YGGFL-EPO standard curve was generated and mutant EPO concentrations determined as described above.

1511 Cell Proliferation Assay. Proliferation assays were performed using the 1511 cell line, a BaF3-derived cell line that has been transfected with a human EPO-R expression plasmid (H. Schneider, personal communication). This cell line is dependent on EPO (or interleukin 3) for survival and proliferation. Cells were maintained in RPMI 1640 medium plus 1 unit of EPO per ml. Prior to use in assay, cells were washed twice in EPO-free medium and starved of EPO in this medium for 2 h. Dilutions of EPO mutants were made in RPMI 1640 medium in a 96-well tissue culture plate (Falcon) and the prestarved 1511 cells added at 20,000 cells/well. The plates were incubated for 16 h before an equal volume of the redox indicator dye Alamar blue (BioSource International, Camarillo, CA) diluted 1:5 in RPMI 1640 medium was added to each well. After 24 h, proliferation curves for EPO mutants were generated by measuring OD_{570nm} - OD_{600nm}. Dose-response curves and EC₅₀ values were generated by using the

program KALEIDAGRAPH (Synergy Software, Reading, PA) by nonlinear least-squares fit to a 4-parameter equation:

$$OD = \frac{(OD_{\max} - OD_{\min})}{1 + \left(\frac{[EPO]}{EC50}\right)^\eta} + OD_{\min}$$

1511 Cell Binding Assay. EPO mutant binding to 1511 cells was determined by competitive displacement of ¹²⁵I-labeled EPO (¹²⁵I-EPO). Prior to the assay, the 1511 cells were washed once in RPMI 1640 medium. Varying concentrations of the EPO variants were mixed with 0.01 μ Ci ¹²⁵I-EPO (386 Ci/mmol; 1 Ci = 37 GBq; Amersham) and 1×10^6 cells in a total volume of 200 μ l. The samples were tumbled for 2–3 h at room temperature and unbound ¹²⁵I-EPO was removed by centrifugation through 0.8 ml dibutyl phthalate at 13,000 rpm for 5 min at room temperature. Cell pellets were isolated by freezing in liquid nitrogen and cutting off the bottom of the sample tubes, then counted in a Beckmann 5500B γ counter. Data was analyzed using the program KALEIDAGRAPH by nonlinear least-squares fit to a simple sigmoidal binding competition model:

$$cpm = \frac{cpm_{\max}}{\left(1 + \frac{[EPO]}{IC50}\right)}$$

ELISA Binding Competition Assay. EPO mutant binding to the extracellular domain of EPO-R (termed EPO binding protein; EPObp) was measured by competitive displacement of biotinylated EPO, detected with a streptavidin/horseradish peroxidase conjugate. Biotinylated EPO was prepared by oxidation of EPO carbohydrates using 10 mM NaIO₄, followed by biotinylation with 10 mM biotin-LC-hydrazide (Pierce) according to the manufacturers instructions. Nunc Maxisorb ELISA plates were coated with mAb 2E12, a nonneutralizing anti-EPO-R antibody (B. van Dyke, personal communication), at 5 μ g/ml in PBS at 4°C overnight. The plates were blocked with 50 mM Tris (pH 8.0) containing 1% (wt/vol) biotin-free BSA for 2 h at room temperature. EPObp was added at a concentration of 20 ng/ml in an assay buffer comprising PBS with 0.1% (wt/vol) BSA and 0.05% (vol/vol) Tween 20 and incubated for 2 h at room temperature. The plates were washed five times with wash buffer [PBS with 0.05% (vol/vol) Tween 20] and 50 μ l of detection mixture (20 ng of biotinylated EPO per ml and 2 μ g of streptavidin/horseradish peroxidase conjugate per ml) added. Samples (50 μ l) of varying concentrations of mutant EPO were immediately added in triplicate and incubation continued for 4 h at room temperature. Samples of WT YGGFL-EPO were loaded on each plate as a standard. Plates were then washed as before and 100 μ l 3,3',5,5'-tetramethylbenzidine (TMB) substrate added, followed by 100 μ l of 2 M H₂SO₄ after 15 min. OD was measured at 450–650 nm, and IC₅₀ values determined by least-squares fit to the equation:

$$OD = \frac{OD_{\max}}{1 + \left(\frac{[EPO]}{IC50}\right)^\eta}$$

after subtraction of background OD values, using the program KALEIDAGRAPH.

RESULTS

Construction and Expression of Mutants. We constructed 18 EPO mutants (Table 1), each with an N-terminal YGGFL epitope tag. Mutant proteins were expressed in serum free medium in 293s cells as described in *Materials and Methods*. Since initial estimates indicated that expression levels were

Table 1. Expression levels of EPO mutants in 293s cells, as determined by BIAcore assay

YGGFL-EPO mutant	3E7 assay, ng/ml
Exp. 1	
R10A	520 ± 40
R14A	480 ± 80
R103A	880 ± 160
S104A	880 ± 40
R150A	960 ± 40
K152A	120 ± 10
Exp. 2	
S9A	760 ± 130
E13A	1000 ± 120
L17A	1700 ± 30
E18A	ND
K20A	1800 ± 60
E21A	1300 ± 90
D136A	800 ± 130
R139A	1400 ± 60
K140A	1400 ± 20
R143A	1600 ± 70
S146A	1300 ± 20

All values were obtained following 10- to 25-fold concentration of tissue culture supernatants and are listed in the table as ng/ml in the original cell supernatant. Expression of WT YGGFL-EPO in two separate experiments was 470 ± 20 ng/ml (experiment 1) and 1900 ± 200 ng/ml (experiment 2), as determined by comparison with WT (nontagged) EPO in a BIAcore assay with the anti-EPO antibody D11 (see *Materials and Methods*). Concentrations of mutants were determined by comparison to WT YGGFL-EPO in a BIAcore assay with the anti-YGGFL antibody 3E7. ND, not determined.

between 0.1 and 2 µg/ml, samples were concentrated ≈10- to 25-fold for subsequent use in assays.

Comparison of YGGFL-EPO with WT EPO and Quantitation of EPO Mutants. First, we compared the activity of the epitope-tagged form of WT EPO with the native form. YGGFL-EPO expressed in 293s cells was quantitated in a BIAcore assay using immobilized D11 (anti-EPO) antibody as described in *Materials and Methods*, with purified WT EPO as a standard. A linear correlation between EPO concentration and rate of binding was observed for concentration values between 50 ng/ml and 40 µg/ml (Fig. 1A). The WT EPO and YGGFL-EPO were assayed using the 1511 proliferation assay and in an ELISA-format binding competition assay as described in *Materials and Methods* (data not shown). Both forms of EPO were found to have identical specific activities in these assays, thus validating the method of quantitation and demonstrating that addition of the N-terminal epitope tag does not impair EPO receptor binding or activation. Next, we quantitated mutant YGGFL-EPO variants in a BIAcore assay with immobilized 3E7 (anti-YGGFL) antibody using the WT YGGFL-EPO as a standard. Again, a linear correlation between EPO concentration and rate of binding was observed, allowing us to quantitate EPO mutants relative to WT EPO with a standard deviation of <20% (Fig. 1B). The results shown in Table 1 illustrate the expression levels observed for each of the EPO variants. Expression of WT YGGFL-EPO varied from ≈0.5 µg/ml to 2 µg/ml between different transfection experiments. The E18A mutant exhibited an unusual BIAcore binding profile compared with the other mutants, and subsequent Western blot analysis revealed that this mutant formed nonreducible high molecular weight aggregates (data not shown). We therefore did not pursue functional analysis of E18A. The K152A mutant was expressed relatively poorly—about 7 times lower than WT YGGFL-EPO.

Cell Proliferation and Receptor Binding Activities of EPO Variants. We examined *in vitro* cell proliferation and receptor

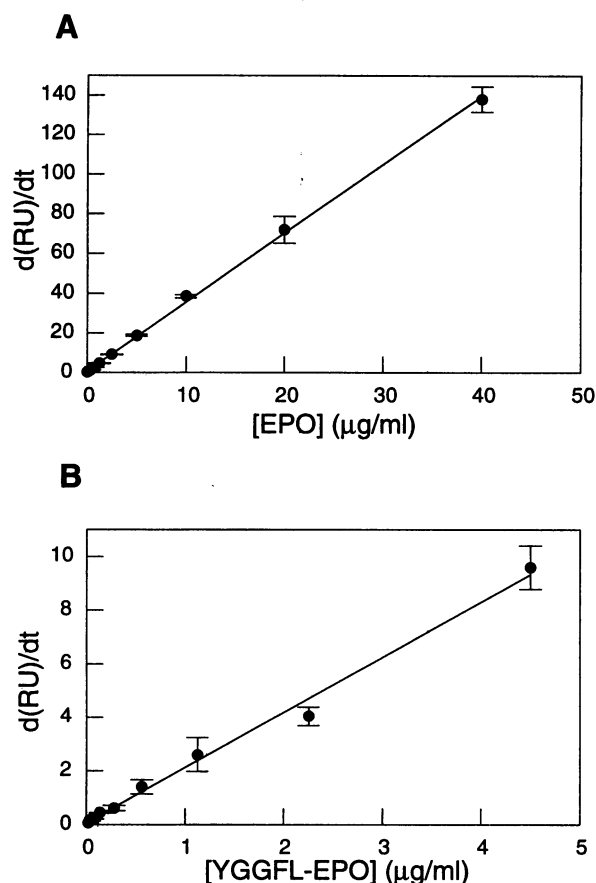


FIG. 1. (A) Standard curve for quantitation of WT YGGFL-EPO in D11 BIAcore assay ($R = 0.999$). (B) Standard curve for quantitation of EPO mutants in 3E7 BIAcore assay ($R = 0.996$). In both assays, concentration of unknown samples was determined by interpolation (see *Materials and Methods*).

binding parameters for each of the EPO mutants by using three assays. First, a proliferation assay using the 1511 cell line was used to determine the ability of each mutant to induce a proliferative signal (Fig. 2). Binding of EPO mutants to soluble EPO-R (EPObp) was also measured in an ELISA-format binding competition assay (Fig. 3A). In this assay, EPObp is

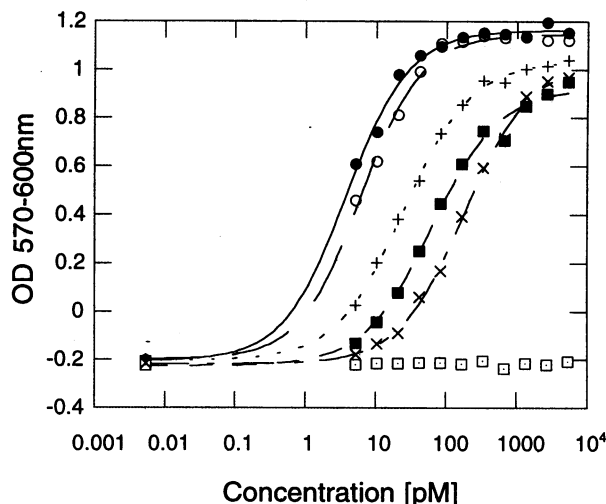


FIG. 2. 1511 proliferation assay for EPO mutants. Some curves have been omitted for clarity; the EC₅₀ values for all mutants are presented in Table 2. ●, WT YGGFL-EPO; ○, R10A; ■, R14A; □, R103A; +, R150A; ×, K152A.

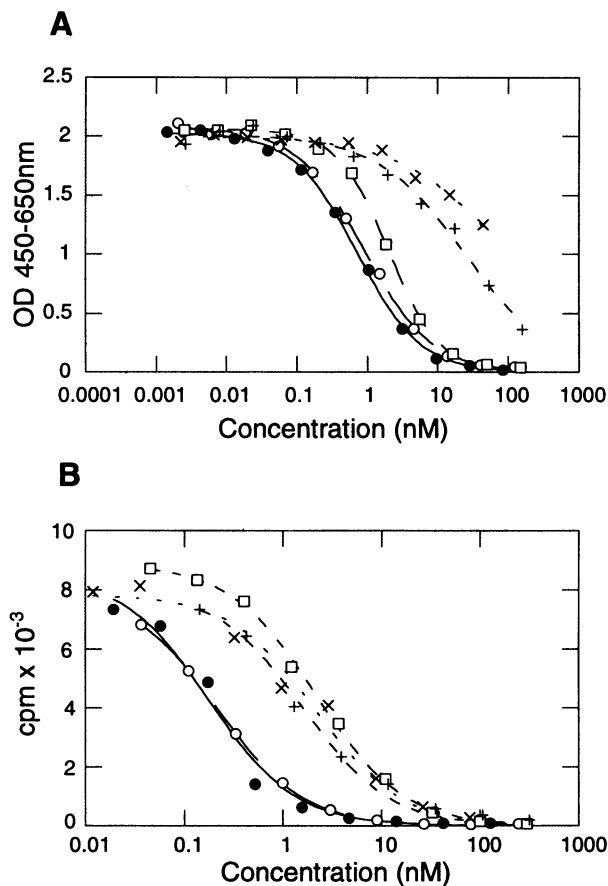


FIG. 3. (A) ELISA binding assay for EPO mutants and (B) 1511 cell binding assay for EPO mutants. Representative curves for WT, R10A, R103A, R150A, and K152A EPO are shown. IC_{50} values for all mutants are presented in Table 2. ●, WT YGGFL-EPO; ○, R10A; □, R103A; +, R150A; ×, K152A.

immobilized by immunocapture in polystyrene ELISA plates. The immobilized EPObp is not free to diffuse (as it is in cell membranes), so we assume that dimerization of EPObp in this assay is greatly impaired compared with dimerization of full-length receptor in cell membranes. Thus, this assay allows us to compare the relative affinities of EPO variants in a 1:1 hormone-receptor complex. For several of the mutants, we also measured cell binding activity in 1511 cells by competitive displacement of ^{125}I -EPO (Fig. 3B). Previous analyses of EPO binding to cellular receptors have typically described the interaction in terms of "high" and "low" affinity binding sites as estimated from Scatchard analysis. However, curved Scatchard plots are also obtained when ligand-induced receptor dimerization occurs, as we believe to be the case for EPO-R. Therefore, we determined an apparent avidity constant for each mutant, equal to the IC_{50} value for cell binding. This avidity constant provides us with a consistent means of comparing the relative effects of each mutant on cell binding, bearing in mind that different mutants may exhibit different propensities for dimerization. The results of these assays are summarized in Table 2.

Seven of the mutants—S9A, R10A, E13A, L17A, E21A, D136A, and R139A—show similar responses to WT EPO in the above assays, suggesting that they do not contribute extensively to EPO bioactivity. Mutants R150A and K152A show significantly decreased receptor binding in the ELISA and in the cell binding assay. However, the proliferation assay also shows a commensurate reduction in activity. In particular, the EC_{50} value for proliferation of the K152A mutant is increased over 30-fold relative to WT EPO. These effects are

Table 2. Binding and proliferation data for YGGFL-tagged EPO and EPO mutants

EPO mutant	EC_{50} in proliferation assay, pM	IC_{50} in cell binding assay, nM	IC_{50} in ELISA, nM
WT	5.5 ± 2.3	0.18	0.72 ± 0.14
S9A	8.1 ± 0.9	ND	1.2 ± 0.1
R10A	6.1 ± 0.5	0.22	0.70 ± 0.2
E13A	9.4 ± 4.6	ND	1.3 ± 0.1
R14A	63 ± 9	1.2	2.4 ± 0.3
L17A	5.1 ± 0.5	ND	1.4 ± 0.2
K20A	7.8 ± 1.2	ND	2.7 ± 0.4
E21A	5.8 ± 1.1	ND	0.9 ± 0.1
R103A	None	2.2	1.6 ± 0.6
S104A	20 ± 3	0.5	1.1 ± 0.1
D136A	12 ± 2	ND	0.8 ± 0.3
R139A	7.0 ± 3	ND	1.0 ± 0.2
K140A	14 ± 1	ND	35 ± 13
R143A	10 ± 2	ND	6.4 ± 0.6
S146A	6.5 ± 2.2	ND	2.7 ± 0.4
R150A	25 ± 2	1.6	20 ± 6
K152A	180 ± 10	2.1	89 ± 16

EC_{50} and IC_{50} parameters were measured by nonlinear regression as described in *Materials and Methods*. EC_{50} proliferation values represent the mean of two independent experiments. ND, not determined.

characteristic of a site 1 mutation, suggesting that R150 and K152 are involved in the initial receptor binding event at the cell surface. The K20A, K140A, R143A, and S146A mutants may also be involved in site 1 binding, since they show increased IC_{50} values in the binding competition ELISA. However, the effects of these four mutations on cell proliferation are relatively small.

In contrast, mutants R103A, S104A, and R14A show relatively small effects on receptor binding in the ELISA, yet significant decreases in proliferative activity are observed. This effect is particularly notable in the case of the R103A mutant, which produces no measurable proliferation at concentrations up to 10 nM. This is consistent with R103, S104, and R14 being in receptor binding site 2. The site 2 EPO mutants are able to bind to the first receptor with near normal affinity, but their ability to dimerize a second receptor at the cell surface is compromised. The R103A, S104A, and R14A mutants also show significantly decreased avidity in the cell binding assay, since they do not form dimeric complexes as readily as WT EPO.

We further analyzed the R103A variant to see if it would antagonize the proliferative effects of WT EPO, since it exhibited no activity in the proliferation assay. Increasing concentrations of R103A were mixed with a fixed concentration (5 pM) of WT EPO and added to 1511 cells as described in *Materials and Methods*. As shown in Fig. 4, antagonistic behavior was observed. The R103A mutant was found to inhibit the proliferative activity of EPO with an IC_{50} value of 5 ± 0.5 nM.

DISCUSSION

One of the critical requirements in performing structure-function mutagenesis studies is accurate quantitation of the mutant proteins. When mutant proteins are expressed in small amounts and are unpurified, ELISA and radioimmunoassay techniques are typically used for quantitation. However, if an antibody recognizes a region of the protein that has been mutated, it may bind with lower affinity and thus give an underestimation of the actual mutant protein concentration. This effect may be somewhat alleviated by use of polyclonal antibodies, but since antibodies in general recognize only a few critical residues on a protein surface (23), some mutant proteins are still likely to be inaccurately quantitated if the mutations are in particularly antigenic regions. We have

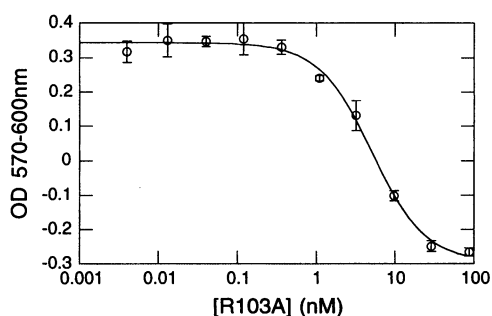
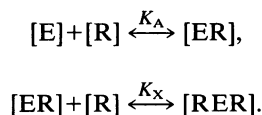


FIG. 4. Antagonism of WT EPO activity by R103A EPO. EPO (5 pM) was added to cells in the presence of increasing concentrations of R103A EPO. The IC_{50} value for R103A EPO was found to be 5.0 ± 0.5 nM. Supernatants from mock-transfected cells exhibited no antagonistic effects (data not shown).

addressed this problem by using an N-terminal YGGFL epitope tag in conjunction with a biosensor assay. We first measured the concentration of WT YGGFL-EPO using an anti-EPO antibody, D11. The YGGFL-EPO was subsequently used as a standard to quantitate mutant proteins in a similar BIAcore assay, this time using the 3E7 (anti-YGGFL) antibody. Addition of an epitope at the N terminus of EPO did not affect the specific activity in proliferation or binding competition assays, in agreement with previously published results (24).

We sought to dissect the mechanism of EPO-R dimerization by constructing a panel of alanine-substitution mutants. The structure of EPO is predicted to be a four-helix bundle (15, 25). Previous mutagenesis studies with EPO (14, 16) have identified residues in both the putative C and D helices which, when changed to alanine, result in EPO analogs with diminished proliferative activity. We chose to study charged residues in the proposed helix D region (D136, R139, K140, R150, and K152) together with S146. R103 and S104 were chosen from the proposed helix C region. We also examined the effects of several residues (S9, R10, E13, R14, L17, K20, and E21) in the putative helix A region. It should be noted, however, that our identification of EPO-R binding sites 1 and 2 is not dependent on the validity of the proposed EPO structure.

We interpreted the results from cell binding and proliferation assays in terms of a sequential dimerization model of binding. Similar models have been described for the interaction of hGH with its receptor (26) and for the interaction of antibodies with cell surface receptors (27). First, we assume that an EPO molecule (E) binds to one receptor molecule (R) via site 1 with affinity constant K_A . We next assume that a second receptor molecule is recruited to the 1:1 EPO/EPO receptor complex (ER) on the cell surface via site 2 of the hormone, forming a complex of one EPO molecule with two receptors (RER). We define the affinity constant for the second receptor binding to the 1:1 complex as K_X , the "crosslinking" constant (27):



We assume further that the amount of proliferative signal is proportional to the amount of dimer on the cell surface. The signal may be saturable—that is, maximal proliferation may be achieved when the fraction of dimeric receptors is still submaximal. In this case, the apparent EC_{50} value for proliferation will be lower than the EPO concentration for half maximal receptor dimer formation. The effects of site 1 affinity (K_A) and site 2 affinity (K_X) on dimer formation in the above model are shown in Fig. 5.

Decreasing the affinity of site 1 leads to an increase in the EC_{50} value for receptor dimerization and consequently an increase in the EC_{50} value for proliferation (Fig. 5A). We observed this behavior for the R150A and K152A mutants. The ELISA data, which measures 1:1 binding of EPO to its receptor, indicate that the initial receptor binding event is impaired for each of these mutants. R150A and K152A were further evaluated for 1511 cell binding and also showed diminished activity in this assay, although the effect was not as pronounced as in the ELISA. We believe that this is due to dimer formation in the cell-based assay, which results in more stable ligand-receptor complexes than in the ELISA. Both mutants have a significantly higher EC_{50} values compared with WT EPO in the 1511 cell proliferation assay. Four mutants (K20A, K140A, R143A, and S146A) also showed weaker binding in the binding competition assay, but relatively small effects on cell proliferation.

Decreasing the affinity of site 2 results in a decrease in the maximum total dimer concentration and a concomitant narrowing of the bell-shaped proliferation curve: hence, in this case too the EC_{50} values for dimer formation and proliferation also increase (Fig. 5B). This is in agreement with our results for the R103A and S104A mutants. Binding of these mutants to EPObp in the ELISA indicates that these mutants have little effect on the initial 1:1 hormone-receptor complex formation. (The small differences that are observed may be due to slight

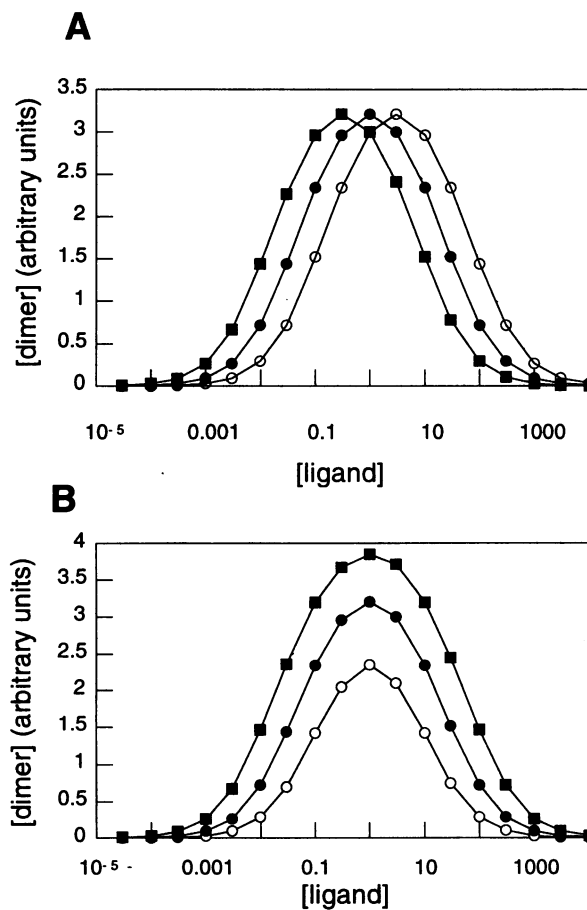


FIG. 5. Graphs showing dimer formation from theoretical dimerization model (see text). These graphs are for qualitative illustration only and are not corrected for ligand depletion effects. In A, K_X is set at 1 and total receptor concentration is set to 10 (in arbitrary units) to show the effect of K_A on receptor dimerization. ■, $K_A = 3$; ●, $K_A = 1$; ○, $K_A = 0.33$. In B, K_A is set at 1 and total receptor concentration is set at 10 to show the effect of varying K_X . ■, $K_X = 3$; ●, $K_X = 1$; ○, $K_X = 0.33$. The amount of dimer formed is a maximum at $[EPO] = 1/K_A$, and each bell-shaped curve is symmetrical about this value.

perturbations in site 1 induced by changes in site 2, or to some small amount of multimeric receptor complex formation in the ELISA. Alternatively, a small amount of binding of WT EPO may bind to EPObp via site 2, which is compromised in the R103A and S104A mutants.) Both R103A and S104A bind to 1511 cells but with lower avidity compared with WT EPO, since the mutants cannot form dimers as readily. However, R103A has no activity in the proliferation assay, and S104A has a significantly increased EC₅₀ value. We believe that removing the R103 side chain impairs site 2 binding to such an extent that the amount of dimer formation is either nonexistent or below the threshold required for cell proliferation. It is important to note that the high local concentration of receptors on the cell surface and the reduced degrees of freedom of these receptors (compared with molecules in solution) may greatly increase the effective affinity of the site 2 interaction (28).

Residue R14 may also be involved in site 2, since the effects of this mutation on proliferation and cell binding are relatively large compared with the increase in IC₅₀ values in the binding competition ELISA. However, this mutant exhibits a 3-fold higher IC₅₀ value than WT EPO in the ELISA, so we cannot exclude some direct or indirect effect of R14 on site 1 binding. The other mutants studied exhibit little difference from WT EPO in our assays, and we thus believe that they are unlikely to be critically involved in the EPO–EPO-R interaction.

The above data strongly suggest that EPO-R activation proceeds via an ordered dimerization mechanism. It should be noted, however, that we cannot formally distinguish a two-site model where the second site has much lower affinity than the first site from a true sequential dimerization model, where the first site is obliged to bind first.

In any stepwise dimerization mechanism, high ligand concentrations should favor formation of 1:1 hormone–receptor complexes at equilibrium and lead to self-antagonism of receptor activation. We have recently shown that this is the case for EPO. Using a [³H]thymidine uptake assay, a downturn in the maximum level of proliferation was observed at EPO concentrations above 3 μM (H. Schneider, personal communication). This is consistent with a transition from dimeric to monomeric receptor complexes at high ligand concentration. Another consequence of a sequential dimerization mechanism is that a ligand which binds only at site 1 should act as an antagonist of the native hormone. We have demonstrated that the R103A mutant has virtually unchanged affinity for site 1 but is incapable of causing signal transduction due to impaired binding at site 2. We investigated the effects of R103A EPO on WT EPO-dependent proliferation and discovered it to be an antagonist (Fig. 4). Under the conditions of this assay (with WT EPO at a concentration of 5 pM) we found that R103A EPO inhibits proliferation with an IC₅₀ value of approximately 5 nM. This finding is striking from the point of view of molecular recognition: removing a single amino acid side chain apparently results in complete loss of site 2 function. Our results are in contrast to those of Wen *et al.* (16), who have reported no such effects in the HCD57 and UT7 cell lines. In this study, the investigators used WT EPO at concentrations up to 50 mU/ml (≈14 pM) and a 5-fold excess of R103A (i.e., ≈70 pM). We did not observe a significant decrease in proliferative response for R103A concentrations up to ≈1 nM, which would explain the lack of antagonism observed by Wen *et al.* (16).

Receptor oligomerization is emerging as an important mechanism in the activation of growth factor receptors (29–31). In particular, the growth hormone subfamily of the class I cytokine receptors (including growth hormone, prolactin, and granulocyte colony stimulating factor) are thought to be activated by ligand-induced homodimerization. Here, we have presented evidence that EPO-R activation proceeds via a sequential dimerization mechanism, similar to that previously described for growth hormone receptor activation (10). We are

currently extending our mutagenesis studies to further our understanding of the EPO–EPO-R interaction, and expect that the R103A antagonist mutant in particular will be an important tool to further dissect the molecular pharmacology of EPO receptor activation.

We thank Amgen Biologicals for providing purified EPO and Dr. Steve Elliott at Amgen Biologicals for providing the D11 antibody. We also thank Drs. Hangjun Zhan and Cyrus Karkaria for supplying us with EPObp and biotinylated EPO, and Dr. Michael Ross for encouragement and support. We are grateful to Dr. Harvey Lodish for critical review of the manuscript.

1. Koury, M. J. & Bondurant, M. C. (1992) *Eur. J. Biochem.* **210**, 649–663.
2. Youssoufian, H., Longmore, G., Neumann, D., Yoshimura, A. & Lodish, H. F. (1993) *Blood* **81**, 2223–2236.
3. Bazan, J. F. (1990) *Proc. Natl. Acad. Sci. USA* **87**, 6934–6938.
4. Yoshimura, A., Longmore, G. & Lodish, H. F. (1990) *Nature (London)* **348**, 647–649.
5. Watowich, S. S., Yoshimura, A., Longmore, G. D., Hilton, D. J., Yoshimura, Y. & Lodish, H. F. (1992) *Proc. Natl. Acad. Sci. USA* **89**, 2140–2144.
6. Watowich, S. S., Hilton, D. J. & Lodish, H. F. (1994) *Mol. Cell Biol.* **14**, 3535–3549.
7. Barber, D. L., Demartino, J. C., Showers, M. O. & D'Andrea, A. D. (1994) *Mol. Cell Biol.* **14**, 2257–2265.
8. Philo, J. S., Aoki, K. H., Arakawa, T., Narhi, L. O. & Wen, J. (1996) *Biochemistry* **35**, 1681–1691.
9. De Vos, A. M., Ultsch, M. & Kossiakoff, A. A. (1992) *Science* **255**, 306–312.
10. Cunningham, B. C., Ultsch, M., De Vos, A. M., Mulkerrin, M. G., Clauser, K. R. & Wells, J. A. (1991) *Science* **254**, 821–825.
11. Cunningham, B. C., Jhurani, P., Ng, P. & Wells, J. A. (1989) *Science* **243**, 1330–1335.
12. Cunningham, B. C. & Wells, J. A. (1989) *Science* **244**, 1081–1085.
13. Cunningham, B. C. & Wells, J. A. (1993) *J. Mol. Biol.* **234**, 554–563.
14. Grodberg, J., Davis, K. L. & Sytowski, A. J. (1993) *Eur. J. Biochem.* **218**, 597–601.
15. Boissel, J.-P., Lee, W.-R., Presnell, S. R., Cohen, F. E. & Bunn, H. F. (1993) *J. Biol. Chem.* **268**, 15983–15993.
16. Wen, D., Boissel, J.-P., Showers, M., Ruch, B. C. & Bunn, H. F. (1994) *J. Biol. Chem.* **269**, 22839–22846.
17. Lin, F. K., Suggs, S., Lin, C. H., Browne, J. K., Smalling, R., Egrie, J. C., Chen, K. K., Fox, G. M., Martin, F., Stabinsky, Z., Badrawi, S. M., Lai, P. H. & Goldwasser, E. (1985) *Proc. Natl. Acad. Sci. USA* **82**, 7580–7584.
18. Jacobs, K., Shoemaker, C., Rudersdorf, R., Neill, S. D., Kaufman, R. J., Mufson, A., Seehra, J., Jones, S. S., Hewick, R., Fritsch, E. F., Kawakita, M., Shimizu, T. & Miyake, T. (1985) *Nature (London)* **313**, 806–810.
19. Kunkel, T. A., Roberts, J. D. & Zakour, R. A. (1987) *Methods Enzymol.* **154**, 367–382.
20. Gorman, C. M., Gies, D. R. & McCray, G. (1990) *DNA Protein Eng. Tech.* **12**, 1–10.
21. Jonsson, U. & Malmqvist, M. (1992) *Adv. Biosensors* **2**, 291–336.
22. Johnsson, B., Lofas, S. & Lindquist, G. (1991) *Anal. Biochem.* **198**, 268–277.
23. Jin, L., Fendly, B. M. & Wells, J. A. (1992) *J. Mol. Biol.* **226**, 851–865.
24. Quelle, D. E., Lynch, K. J., Burkert-Smith, R. E., Weiss, S., Whitford, W. & Wojchowski, D. M. (1992) *Protein Expression Purif.* **3**, 461–469.
25. Bazan, J. F. (1990) *Immunol. Today* **11**, 350–354.
26. Ilondo, M. M., Damholt, A. B., Cunningham, B. C., Wells, J. A., De Meyts, P. & Shymko, R. M. (1994) *Endocrinology* **134**, 2937–2403.
27. Perelson, A. (1984) in *Cell Surface Dynamics: Concepts and Models*, eds. Perelson, A. S., DeLisi, C. & Wiegel, F. W. (Dekker, New York), pp. 223–276.
28. Grasberger, B., Minton, A. P., DeLisi, C. & Metzger, H. (1986) *Proc. Natl. Acad. Sci. USA* **83**, 6258–6262.
29. Wells, J. A. (1994) *Curr. Opin. Cell Biol.* **6**, 163–173.
30. Heldin, C.-H. (1995) *Cell* **80**, 213–223.
31. Davies, D. R. & Wlodawer, A. (1995) *FASEB J.* **9**, 50–56.